



Accepted Article

Title: Preparation and Characterization of some new one-dimensional organic-inorganic hybrid materials based on Sb

Authors: George A Mousdis, Nikolaos - Minas Ganotopoulos, Hamdi Barkaoui, Younes Abid, Vassilis Psycharis, Aikaterini Savvidou, and Catherine Raptopoulou

This manuscript has been accepted after peer review and appears as an Accepted Article online prior to editing, proofing, and formal publication of the final Version of Record (VoR). This work is currently citable by using the Digital Object Identifier (DOI) given below. The VoR will be published online in Early View as soon as possible and may be different to this Accepted Article as a result of editing. Readers should obtain the VoR from the journal website shown below when it is published to ensure accuracy of information. The authors are responsible for the content of this Accepted Article.

To be cited as: *Eur. J. Inorg. Chem.* 10.1002/ejic.201700277

Link to VoR: <http://dx.doi.org/10.1002/ejic.201700277>

Preparation and Characterization of some new one-dimensional organic-inorganic hybrid materials based on Sb

George A. Mousdis^{*, [a]} Nikolaos - Minas Ganotopoulos,^[a] Hamdi Barkaoui,^[b] Younes. Abid^[b] Vassilis Psycharis^[c], Aikaterini Savvidou^[c] and Catherine P. Raptopoulou^[c]

Abstract:

The rise of lead halide perovskites as light harvesters has stunned the photovoltaic community, due to high efficiencies achieved. The hybrid metal halide perovskites, due to unique optical and electronic properties and the corresponding application in optoelectronic devices are a hot topic of academic research. Although the Pb and Sn hybrids are used in most cases, they present stability and toxicity problems. For these reasons other similar compounds with other metals were investigated. Sb based hybrid perovskites are good alternatives of the Pb based analogues for the photovoltaic and other applications. In this paper four novel organic-inorganic hybrid compounds of the general formula $[\text{CH}_3\text{SC}(\text{NH}_2)_2]_2\text{SbA}_5$, (A=I, Br, Cl, and Cl/Br) were successfully synthesized. Their structure consists of corner sharing SbX_6 octahedra forming zigzag chains with the amine located in the free cavities between chains. Their structure, optical and vibronic properties were studied. DFT calculations were made in order to compare the results with the experimental findings and gain an insight of the properties of these new compounds.

Introduction

During the last two decades, a great attention has been devoted to the class of organic-inorganic metal halides based perovskites with the general formula $\text{C}_x\text{M}_y\text{A}_z$ (C = organic amine or diamine, M= Pb, Sn, Bi, Sb or other metal and A=I, Br, Cl), due to their special structural features and physical properties, including interesting optical and electronic properties [1], ideal thermal and mechanical stability, non linear optical effects [2] and efficient luminescence [3].

The anionic sublattices of these materials are built up by distorted anionic $[\text{MA}_6]^\ominus$ octahedra [4]. These octahedra can be isolated or linked by corners, edges, or faces leading to low dimensional inorganic framework. The crystal packing is directed by the interactions between the components constituting the solid such as hydrogen bonding, Van Der Waals, and electrostatic interactions, and can be controlled by the organic cation size, shape, characteristic groups, charge, steric

encumbrance etc. The organic moiety can be used as physical and electronic barrier, contributing to original electrical and optical behaviour [5]. A wide range of organic amines can be used, including many alkyl and simple aromatic and depending from their size and functionality different structures can be achieved.

Recently $(\text{CH}_3\text{NH}_3)\text{PbA}_3$ has emerged as a remarkable photovoltaic absorber material demonstrating power conversion efficiencies (PCE) above 20% [6]. Moreover the application of hybrid perovskites have been extended with superlative results to light-emitting devices opening new frontiers for perovskite based lasers [7], light-emitting diodes (LEDs) [8], and field-effect transistors (FETs) [9]. However, the intrinsic instability and potential toxicity of these materials make them less than ideal candidates for large-scale deployment. Therefore, great efforts are being made to identify alternative lead free materials with comparable properties and energy conversion efficiency [10]. A promising family are the perovskites based on trivalent metals that also have high exciton binding energy, are stable to humidity and they are not toxic [11]. Two recent examples are the layered $\text{Cs}_3\text{Sb}_2\text{I}_9$ [11] and $\text{A}_3\text{Bi}_2\text{I}_9$ [12] (A: CH_3NH_3 or Cs), although the yield are still very low, similar materials can increase it significantly. The antimonium-halogen based hybrids compounds have been extensively investigated since they have demonstrated a propensity for forming a variety of crystalline structure by self assembling from suitable solutions mixtures [13]. It has been shown that their structures can vary considerably, ranging from systems based on isolated (0-D) inorganic polyhedral to ones (1-D) containing extended chains [4], right up to two-dimensional (2-D) networks [14]. Due to their semiconducting character, their low dimensional structures and the high dielectric constants difference, of the organic and inorganic part, strong quantum and dielectric confinement effects appear. So stable excitons with large binding energies are formed and confined in the inorganic part giving rise to interesting optical and electronic properties.

In the present paper the synthesis structure and optical properties of four antimonium based hybrid perovskites with the $\text{CH}_3\text{SC}(\text{NH}_2)_2^+$ cation are described. The results are compared with those observed from similar Low Dimensional (LD) compounds based on inorganic units.

Results and Discussion

Morphology of materials: The compounds studied herein were prepared in a pure single crystal form. The crystals were large enough for X-ray crystal structure determination and investigation of their physical properties.

Synthesis: The synthesis was done by refluxing the amine salt and Sb_2O_3 in the corresponding hydrohalogenic acid. But in the case of salt with Cl we use the bromine salt of amine expecting that the product will be only with Cl due to excess of it, as in

[a] G. A., Mousdis, N-M, Ganotopoulos.
National Hellenic Research Foundation Theoretical and Physical Chemistry Institute. Vass. Constantinou Ave., 48 116-35 Athens Greece E-mail: gmousdis@eie.gr
<http://www.eie.gr/nhrfi/institutes/tpci/researchteams/mspc/mspc-ld-organicconductors-gr.html>

[b] H. Barkeoui, Y. Abid
Laboratoire de Physique Appliqué, Faculté des Sciences de Sfax, University of Sfax, BP 1171, Sfax, Tunisia

[c] V. Psycharis, A. Savvidou, C.P. Raptopoulou
Institute of Nanoscience and Nanotechnology NCSR, Demokritos, 15310 Aghia Paraskevi, Attikis, Greece

Supporting information for this article is given via a link at the end of the document.

FULL PAPER

WILEY-VCH

previous preparations [15]. Instead from the structural analysis, as well as, from the chemical analysis we found that the salt has a $\text{Cl}_{3.86}\text{Br}_{1.14}$ analogy. To obtain the Cl salt, we synthesize the Cl salt of the amine and we prepared the Sb salt by a similar to the other salts method.

Crystal Structure: The stoichiometric formula and the content of the asymmetric unit of the cell for all the compounds is $[\text{CH}_3\text{SC}(\text{NH}_2)_2]_2\text{SbA}_5$ [A= I for **1**, Br for **2** (Cl/Br) for **3** and Cl for **4**]. Compound **3** contains a small amount of Br due to the synthetic procedure. The sites of Cl and Br atoms are in disorder and they are partially occupied, 77.2% and 22.8%, by the corresponding atoms. All four compounds crystallize in the monoclinic $P2_1/n$ space group and the **1**, **2**, **3** are isomorphous. Structural details for all studied compounds are given in Table-1 and Tables S1, S2 and S3 of supporting information. In the case of compounds **1**, **2** and **3** there are two symmetry independent cation molecules in the asymmetric part of the cell (Fig. 1a). The anionic part of the structure consists of SbA_6^{-3} units, which are distorted octahedra forming one dimensional zig-zag chains along b-axis through corner sharing (Fig. 1b). The Sb–I bond lengths in the distorted SbI_6 octahedra vary from 2.8091(0) to 3.3439(1) Å, with the bridging bond distances Sb1-A1 , $\text{Sb1-A1}''$, being the longest (Table S2 and Fig. 1b). Almost all halogen sites in compound **3** (except A4) are partly substituted by Br atoms. The anionic chains are packed in layers parallel to the (001) plane which are stacked along the c-axis, as shown in Figure 1c. There are short conducts among the halogen atoms within these layers i.e. 3.927, 3.774 and 3.887 Å, for compounds **1**, **2** and **3**, respectively, which are longer than the sum of the van der Waals radii for Cl and Br (3.5 and 3.7 Å) but shorter for that of I (3.96 Å). Compound **4** also crystallizes in the $P2_1/n$ space group with the double of the cell volume of the other three (Tables 1 and S1) and the structural model has been obtained from a twin crystal (for details in Structure determination section). It has the same stoichiometric formula as the other three, but in the asymmetric unit of the cell exist the double of the content as compared to them i.e. there have been found two SbA_5^{-2} and four $\text{CH}_3\text{SC}(\text{NH}_2)_2^+$ symmetry independent units. In compound **4** the two SbA_5^{-2} symmetry independent units, form two different zig-zag chains of corner sharing SbCl_6 octahedra and both are extended along the b-axis (Fig. 1d). In **4**, the angle between the plane defined by the chains formed by Sb1 with the plane defined by the chains formed by Sb2 cations is $78.895(8)^\circ$ (Fig. 1e). Successive neighbouring chains are packed in the same way forming the same angle among each other and this results in the formation of an extensive characteristic tweed structure, Fig. 2c. In the case of compounds **1**, **2** and **3** neighbouring chains are stacked parallel to each other as in Fig. 1c. The bending angle of the bridging halogen atoms take higher values in the case of **4** ($\text{Sb1-Cl1-Sb1}''$: $173.35(7)^\circ$, $\text{Sb2-Cl6-Sb2}''$: $178.43(10)^\circ$, Table S2) and ($164.152(9)^\circ$, $159.418(10)^\circ$ and $154.5(5)^\circ$ for **1**, **2**, **3** respectively, Table S2).

The cations fill the space between the layers of chains and are attached to them through an extensive net of hydrogen bonds. In compounds **1**, **2** and **3** the cations possessing the S1 (cation-1) and S2 (cation-2) atoms (Fig. 1a) form pairs of the same species and fill the space indicated with red and cyan lines respectively in Fig. 1c. The arrangement of the cations and the hydrogen bonds developed between them and the anionic chains for the three compounds are shown in Fig. 2a and those of compound **4** in Fig. S1. In the case of compound **4** S...S contacts are

developed among pairs of cations (Fig. S1), more specifically the S1...S3 and S2...S4 contacts take values 3.498 (4) and 3.464(4) Å, which are well below the sum, 3.6 Å, of their van der Waals radii. A part of the 3D architecture for the three structures is shown in Fig. 2b and the respective view for compound **4** in Fig. 2c. Hydrogen bond values and their respective labels for all studied compounds are listed in Table S3.

Table 1. Crystallographic parameters of prepared compounds

Compound	1	2	3	4
Formula	$\text{C}_4\text{H}_{14}\text{I}_5\text{N}_4\text{S}_2$ Sb	$\text{C}_4\text{H}_{14}\text{Br}_5\text{N}_4\text{S}_2$ Sb	$\text{C}_4\text{H}_{14}\text{Br}_{1.14}\text{Cl}_{3.86}\text{N}_4\text{S}_2\text{Sb}$	$\text{C}_8\text{H}_{28}\text{Cl}_{10}\text{N}_8$ S_4Sb_2
Space group	$P 2_1/n$	$P 2_1/n$	$P 2_1/n$	$P 2_1/n$
Z	4	4	4	4
a (Å)	12.1322 (3)	11.4258 (4)	11.2361 (2)	20.6986(4)
b (Å)	9.2693 (2)	8.9079 (3)	8.7604 (2)	8.4146(2)
c (Å)	18.3339 (4)	17.3627 (5)	16.8540 (3)	20.8254(4)
β	$93.630(1)^\circ$	$92.225(1)^\circ$	$91.843(1)^\circ$	$111.7230(11)^\circ$
V (Å ³)	2057.64(8)	1765.84(10)	1658.13 (6)	3369.58(12)

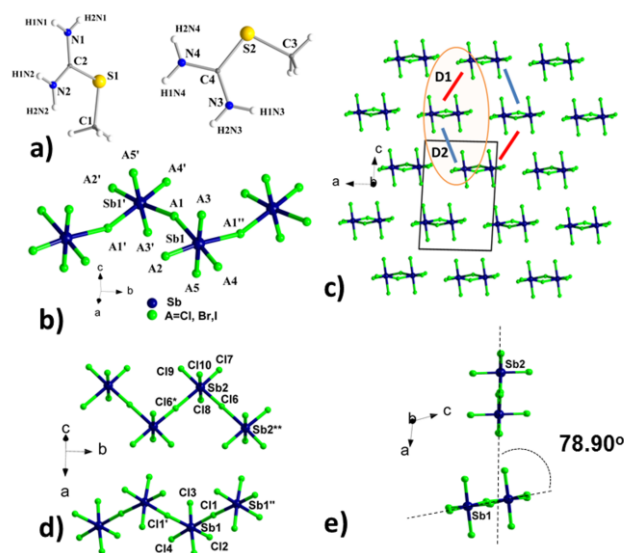


Figure 1. Compounds **1,2,3** a) Labelling scheme of the two symmetry independent cations (cation-1, possesses atom S1 and cation-2 possesses atom S2) presented in the unit cell b) Zig-Zag chains along b-axis formed through corner sharing of distorted SbA_6^{-3} octahedra. c) Packing arrangement of chains (view down the $-b$ axis). D1 (red lines) and D2 (blue lines) label the lattice sites of cation-1 and cation-2 respectively. Compound **4** d) Arrangement of symmetry independent zig-zag chains along the b axis e) Relative orientation of neighbouring chains presented along $-b$ axis. Only the Sb and A (=Cl or Br, Br and I) atoms are shown. Symmetry code: (*): $1.5-x, -0.5+y, 0.5-z$; (**): $1.5-x, 0.5+y, 0.5-z$; (**'): $0.5-x, -0.5+y, 0.5-z$; (**''): $0.5-x, 0.5+y, 0.5-z$.

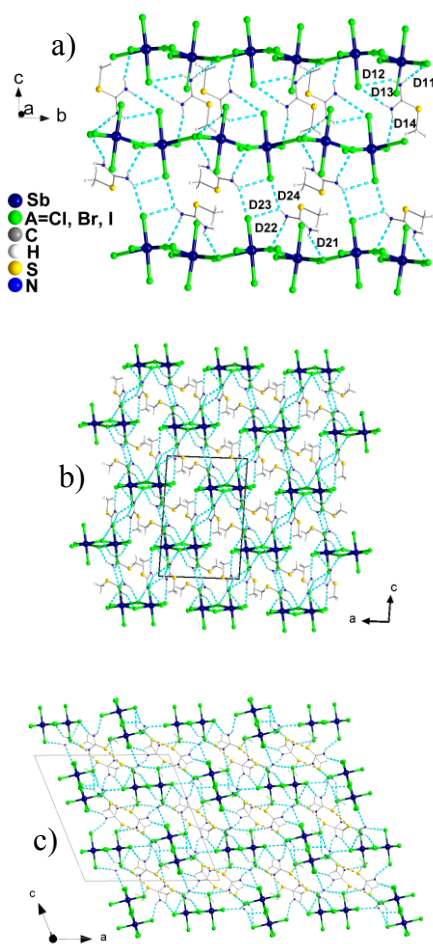


Figure 2. Compounds **1, 2, 3.** a) Side view of chains interacting through hydrogen bonds with the cations. Dashed cyan lines indicate hydrogen bonds. The values for the hydrogen bonds corresponding to the given labels are listed in Table S3 b) A part of the 3D plot for the three structures is shown projected down the $-b$ axis. c) The respective 3D plot for Compound **4.**

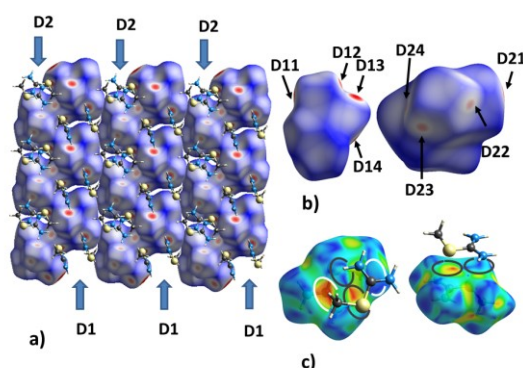


Figure 3. Compounds **1,2,3.** a) Hirshfeld surface of layers of chains of SbA₆⁻³ units parallel to the (001) planes, mapped with d_{norm} values. The labels D1 and D2 indicate the series of pairs of cation-1 and pairs of cation-2 respectively and which are distributed above the layer of anionic chains. b) Hirshfeld surfaces mapped with d_{norm} values for cation -1 (left) and cation -2 (right). The hydrogen bonds corresponding to the given labels are listed in Table S3. c) Pairs of the same cations presented in mixed ball & stick models and Hirshfeld surfaces mapped with S index values. The circled areas indicate their conduct points. The left image are for those pairs possessing S1 sulfur atoms and the right image are for those possessing S2 sulfur atoms.

The investigation of the intermolecular interactions and crystal packing using the Hirshfeld surface analysis method [16], unveil interesting characteristic of the structures. Fig. 3a represents the zig-zag chains formed by SbA₆⁻³ units in compounds **1,2,3** arranged in layers parallel to the (001) plane using the Hirshfeld surface representation, mapped with the d_{norm} values. The areas where the intermolecular contacts are shorter than the sum of their Van der Waals radii are highlighted in red, on a d_{norm} decorated surface, longer contacts are shown in blue and contacts around the sum of Van der Waals radii in white. The red areas on the surfaces presented in Fig. 3a are the interaction points of the halogens with the hydrogen atoms of cations as have been discussed previously. It is clearly seen that the chains within the (001) plane are almost “touching” each other, as the halogen...halogen contacts are shorter (for I) or little longer (for Cl and Br) than the sum of their van der Waals radii of the corresponding atoms in the layer (see discussion above). Above from these layers of chains “valleys” are formed arranged in a zig-zig way following to the anionic chains lying below. Pairs of cations possessing S1 and pairs of cations possessing S2 sulfur atoms reside within these valleys, are attached to these layers through hydrogen bonds and form the D1 and D2 series of pairs of cations shown in Fig. 3a.

The Hirshfeld surfaces mapped with d_{norm} values for both cations in compounds **1,2**, and **3** are shown in Fig. 3b, where the red areas indicate the hydrogen bond contact areas with the corresponding halogen atoms (values and labels for the corresponding hydrogen bonds are given in Table S3). Both cations present the same features on these surfaces and the main difference concerns the volumes occupied by each cation in the three studied structures. The molecular volumes for cations -1 and -2 calculated by Hirshfeld surface analysis are 113.98 Å³ and 112.10 Å³ for compound-1 (I), 111.39 Å³ and 108.74 Å³ for compound-2 (Br) and 112.28 Å³ and 110.54 Å³ for compound-3 (only Cl atoms have been considered in the calculations in this case) respectively. Fig. 3c presents centrosymmetrically related pairs of cations possessing S1 (left image) and pairs of cations possessing S2 (right image) sulphur atoms. One of the molecules of each pair is presented with Hirshfeld surface decorated with the Shape index, S and the white and dark gray circled regions (Fig. 3c) indicate complementary hollows (red) and bumps (blue) regions where neighbouring molecular Hirshfeld surfaces touch one another. In both images of Fig. 3c the second molecule is presented in ball and stick model. In the case of pairs of cations possessing S1 atoms (left image) they touch each other at two points, at one point is through hydrogen atoms at the methyl end of one cation with the carbon atom at the amine end (white circles) of the other cation and the other point is through an hydrogen atom at the amine end (dark gray circles) of one cation with the sulfur atom of the other cation. In the case of pairs of cations possessing S2 atoms (right image) they touch each other at one point i.e. the carbon atom of the amine end of one cation touches the sulfur atom of the other and vice versa.

The Hirshfeld surfaces mapped with d_{norm} values for the four symmetry independent cations in compound **4** are shown in Fig. S2, where in addition to the hydrogen bond contacts the S...S contacts are also clearly seen. The volumes of the corresponding four cations in compound **4** are 117.46, 115.91, 115.43 and 115.82 Å³.

FULL PAPER

WILEY-VCH

As it can be seen by the fingerprint plots of the compounds (Fig. S3 and S4) there is an asymmetric distribution of the different features, which is a clear evidence that the interactions concern different species. The $H\cdots A$ ($A = I, Br, Cl$) type of interactions are the strongest and the more abundant (more than 40%, of all the interactions for each cation) in all studied compounds (Figure S3 and S4). The van der Waals-type $H\cdots H$ and $S\cdots H$ interactions, which give contribution in the range 19.1-26.6 and 11.9-16.1% for the three structures, are weak and provide little stabilization. The two C-N bond lengths are almost equal (Table 2 at supporting info), indicating that the cations have a resonance structure $[CH_3SC(\dots NH_2)_2]$.

Hydrogen bond interactions in the structure of Lead based halide perovskites have been considered that influence the tilting angles of Lead octahedra and through these the optical band gap [17]. They also influence the geometric characteristics of $SbBr_5^{-2}$ units forming zig-zag chains in structures with small sized organic cations [18]. Using the distortion parameters Δ and σ^2 [18a], (Table S2) in our case, both indicate an increase in distortion upon I replacement with Br and Cl, (compounds **1**, **2** and **3** respectively). In the case of compound **4** the octahedra are relaxed as these parameters take small values [Table S2]. The variation in the values of these parameters has been correlated with the hydrogen bonds developed among the halide atoms and the small organic cations [18a]. It is characteristic to note that the A2 halide atoms (I2, Br2 and Cl2 in compounds **1**, **2** and **3**) which do not participate in any hydrogen bond have a short Sb-A2 bond length (Table S2). In the case of compound **4** the Cl2 atom which does not participate in any hydrogen bond shows a short Cl2-Sb1 bond Cl-Sb1 (2.431 Å, Table S2) and the Cl7 which do participate in a long hydrogen bond [2.79 Å] show also a short Sb-Cl7 distance (2.424 Å, Table S2). In contrast when there are short hydrogen bonds the Sb-A bonds are longer e.g. for the compound **1**, N2—H1N2 \cdots I5 is 2.83 Å (Table S3) and Sb1-I5 is 3.0780 Å (Table S2).

The DFT optimized geometries of the compounds are presented in Fig. S5.

XRPD measurement of a film prepared from spin coating of a CH_3CN solution of compound **1** (Fig. S6) shows that the reflections from (10-1) family of planes are very intense indicating that the grains are oriented parallel to these planes on the glass substrate. The inset in Fig. S6 gives the relative orientation of chains with respect to the substrate.

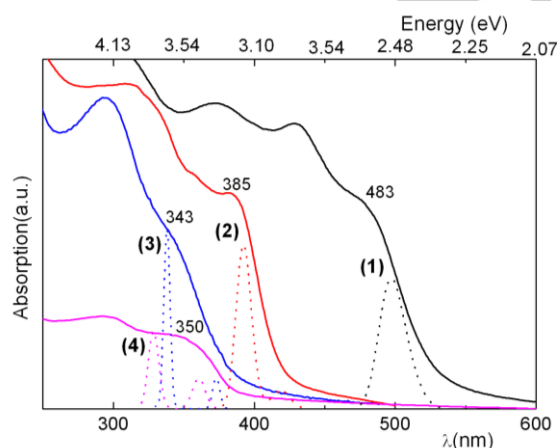


Figure 4: Optical absorption spectra of thin films of compounds **1**, **2**, **3**, **4** at room temperature Experimental (straight lines) and calculated (dotted lines). X values at nm (lower axis) and at eV (higher axis)

UV-Vis Spectra

Fig. 4 shows the room temperature optical absorption spectra of thin deposits of compounds and the calculated absorption bands, for the prepared compounds. As we can see in the figure the salts showing excitonic peaks at 483, 385, 343 and 350 nm for the I, Br, $Br_{1.14}Cl_{3.86}$ and Cl compounds respectively. The calculated band gaps from the Tauc plots of the absorbance data (Fig. S7) was found to be 2.41, 3.03, 3.34 and 3.24 eV for compounds **1**, **2**, **3**, **4** respectively, assuming a direct band gap (Table 2).

	Gap		Shift	2 nd transition		Shift
	Experiment	Theory		Experiment	Theory	
(1)	2.41	2.43	0.02	2.59	2.5	0.09
(2)	3.03	2.96	0.07	3.22	3.16	0.06
(3)	3.34	3.32	0.02	3.61	3.66	0.05
(4)	3.24	3.43	0.21	3.46	3.77	0.31

In the compounds $[H_3N(CH_2)_6NH_3]SbX_5$ ($X = I, Br$) with a similar zig-zag 1D structure the excitonic peaks occur almost at the same region for the Br (392 nm) but at significantly higher values for the I (513 nm) [4]. Although many similar compounds have been prepared, according to our knowledge there is no information about their optical properties with the exception of the layered $Cs_3Sb_2I_9$ with an almost 2D structure, that has a band gap of 2.05 eV (absorption peak at ~ 600 nm) [11].

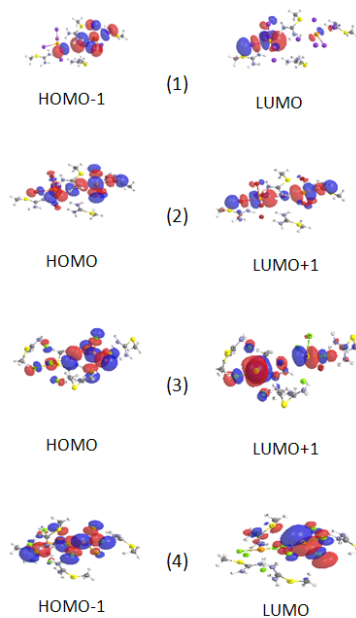


Figure 5: Electronic transitions in compounds (1), (2), (3) and (4) (blue: negative charges, red: positive charges).

The theoretical calculation predicts absorption peaks at 2.5 eV, 3.16 eV, 3.66 eV and 3.77 eV, for compounds (1), (2), (3) and (4) respectively. These calculated bands correspond to

FULL PAPER

WILEY-VCH

giving us the ability to prepare tailor made compounds by combining 2 or even 3 halogens. When dealing with compounds (**1**), (**2**) and (**3**), TDDFT calculations show a pretty good agreement with the experimental data, i.e. I.R., Raman and UV-vis spectra. However, cluster simulation does not fit well with the compound (**4**) and crystal computation will be needed to well determine the electronic properties of this compound.

In any cases more specified studies are required such as computation of the band structure and detailed study of films structure and properties. Moreover appropriate molecular design will be necessary to improve the material's properties and solar cell performance filling the gap with the state-of-the-art Pb-based perovskite devices..

These new materials may find applications also in other perovskite devices such as light-emitting diodes and photodetectors.

Experimental Section

Synthesis

Starting materials: The following starting materials were used without further purification. Antimony (III) oxide (Ferk 30199), hydroiodic acid 57% (Merck 341), hydrobromic acid 47% (Merck 304), hydrochloric acid 25% (Merck 312). The preparation of amines was described in a previous paper [15]. The $\text{CH}_3\text{SC}(\text{NH}_2)_2\text{I}$ and $\text{CH}_3\text{SC}(\text{NH}_2)_2\text{Br}$ was prepared by a previous published method [15].

The $\text{CH}_3\text{SC}(\text{NH}_2)_2\text{Cl}$ was prepared by refluxing a solution of 7.6 g (13 mmol) of thiourea and 4 ml of HBr in 30 ml methanol for 24 h. The solution was condensed to 5 ml and cooled at 0 °C to give 1 g of a white crystalline precipitate. The precipitate was filtered off and washed with 2ml of cold methanol to give 1g (9 mmol) (Yield 70%).

$[\text{CH}_3\text{SC}(\text{NH}_2)_2]_2\text{SbI}_5$, [1]: 1.45 gr of Sb_2O_3 (5 mmole) and 4.36 g of $\text{CH}_3\text{SC}(\text{NH}_2)_2\text{I}$ (20 mmole) were dissolved in 5 ml of HI the solution was refluxed for 2 hours. The solution was concentrated to 1 ml and cooled at 0 °C for 12h to give red crystals. The crystals were filtrated and left at vacuum for 8 hours to dry and remove any traces of HI. It gave 4.1g (4.36 mmole) (Yield 43,6%). (mp: 175° C)

$[\text{CH}_3\text{SC}(\text{NH}_2)_2]_2\text{SbBr}_5$, [2]: 1.45 gr of Sb_2O_3 (5 mmole) and 3.42 g of $\text{CH}_3\text{SC}(\text{NH}_2)_2\text{Br}$ (20 mmole) were dissolved in 5 ml of HBr the solution was refluxed for 2 hours. After cooling at 0 °C for 12h 1.1 g of yellow crystals were formed. The crystals were filtrated and left at vacuum for 8h to dry and remove any traces of HBr. The filtrate was condensed to <1ml and after cooling at 0° gave another 2g of product. (mp: 180-182° C) (Yield 44%)

$[\text{CH}_3\text{SC}(\text{NH}_2)_2]_2\text{SbCl}_{3.86}\text{Br}_{1.14}$, [3]: 1.45 g of Sb_2O_3 (5 mmole) and 3.42 g of $\text{CH}_3\text{SC}(\text{NH}_2)_2\text{Br}$ (20 mmole) were dissolved in 5ml of HCl and refluxed for 10 min. the solvent was evaporated slowly to give 2.13 g (4 mmol) of white crystals. (Yield 40%) (mp: 113° C)

$[\text{CH}_3\text{SC}(\text{NH}_2)_2]_2\text{SbCl}_5$, [4]: 1.45 g of Sb_2O_3 (5 mmole) and 2.24 g of $\text{CH}_3\text{SC}(\text{NH}_2)_2\text{Cl}$ (20 mmole) were dissolved in 5ml of HCl and refluxed for 10 min. the solvent was evaporated slowly to give 2.31 g of white crystals (4.8 mmole) . (mp: 173 C) (Yield 48%)

Characterization

X-ray crystal structure determination. Important crystallographic data for the studied samples are listed in Table 1 (and Table S1, S2 and S3 at supporting information). An orange crystal of **1** (0.04, 0.09, 0.24 mm) a

yellow one of **2** (0.09, 0.12, 0.40 mm), a colorless one of **3** (0.12, 0.16, 0.23 mm), and also a colorless one of **4** (0.06, 0.07, 0.33 mm) was taken from the mother liquor and immediately cooled to -113 °C. Diffraction measurements were made on a Rigaku R-AXIS SPIDER Image Plate diffractometer using graphite monochromated Mo K α radiation. XRPD measurements for the film and the powder were made on a D500 Siemens diffractometer using CuK α radiation at room temperature. Data collection (ω -scans) and processing (cell refinement, data reduction and Empirical absorption correction) were performed using the CrystalClear program package [24]. The structures were solved by direct methods using SHELXS-97 [25a] and refined by full-matrix least-squares techniques on F^2 with SHELXL ver.2014/6 [25b]. Further experimental crystallographic details for **1**: $2\theta_{\text{max}} = 54.0^\circ$; reflections collected/unique/used, 21040/4477 [$R_{\text{int}} = 0.0298$]/ 4477; 190 parameters refined; $(\Delta/\sigma)_{\text{max}} = 0.002$; $(\Delta\rho)_{\text{max}}/(\Delta\rho)_{\text{min}} = 0.940/-0.592 \text{ e}/\text{Å}^3$; $R1/wR2$ (for all data), 0.0239 / 0.0378. Further experimental crystallographic details for **2**: $2\theta_{\text{max}} = 54.0^\circ$; reflections collected/unique/used, 36867/3856 [$R_{\text{int}} = 0.0384$]/ 3856 parameters refined 201; $(\Delta/\sigma)_{\text{max}} = 0.002$; $(\Delta\rho)_{\text{max}}/(\Delta\rho)_{\text{min}} = 0.730/-0.701 \text{ e}/\text{Å}^3$; $R1/wR2$ (for all data), 0.0194/0.0359. Further experimental crystallographic details for **3**: $2\theta_{\text{max}} = 54.0^\circ$; reflections collected/unique/used, 30652/3619 [$R_{\text{int}} = 0.0249$]/3619 parameters refined 241; $(\Delta/\sigma)_{\text{max}} = 0.065$; $(\Delta\rho)_{\text{max}}/(\Delta\rho)_{\text{min}} = 0.849/-0.352 \text{ e}/\text{Å}^3$; $R1/wR2$ (for all data), 0.0188/0.0423. At the early stage of refinement for **3** the temperature factor values for Cl1, Cl2 Cl3 and Cl5 atoms were too low and in the difference Fourier Maps close to these atoms additional electron density was calculated (up to $5 \text{ e}/\text{Å}^3$). To overcome these findings Br atoms were included in the model at disordered sites and the final occupancy values are: Cl1/Br1: 0.607(2)/0.393(2); Cl2/Br2: 0.796(2)/0.204(2); Cl3/Br3: 0.719(2)/0.281(2); Cl5/Br5: 0.735(2)/0.265(2). Further experimental crystallographic details for **4**: as the a and c axes are approximately equal the crystal presents pseudomerohedral twinning with an additional 2-fold axis parallel to the [10-1] crystallographic direction i.e. the twin law is (0,0,-1/0,-1,0/1,0,0) and the refinement was performed with hk15 data file and the BASF parameter was refined to the value 0.178(2), $2\theta_{\text{max}} = 54.0^\circ$; reflections collected/unique/used, 62804/7686 [$R_{\text{int}} = 0.044$]/ 7319; parameters refined 321; $(\Delta/\sigma)_{\text{max}} = 0.000$; $(\Delta\rho)_{\text{max}}/(\Delta\rho)_{\text{min}} = 0.691/-0.914 \text{ e}/\text{Å}^3$; $R1/wR2$ (for all data), 0.0672/0.0981. All hydrogen atoms in **1** and **4** were either located by difference maps and were refined isotropically or introduced at calculated positions as riding on bonded atoms. In **2** and **3** were located by difference maps and were refined isotropically. All non-hydrogen atoms for all structure were refined anisotropically. Plots of the structure were drawn using the Diamond 3 program package [25c]. The packing of the complexes in the crystal structures was further investigated with the Hirshfeld surface (HS) analysis method using the CrystalExplorer package [26].

CCDC 1537196, 1537197, 1537198, 1537199 contain the supplementary crystallographic data for the compounds **1**, **2**, **3** and **4** respectively. These data can be obtained free of charge via www.ccdc.cam.ac.uk/contents/retrieving.html (or from the Cambridge Crystallographic Data Centre, 12 Union Road, Cambridge CB21EZ, UK; fax: (+44) 1223-336-033; or deposit@ccdc.cam.ac.uk).

Optical absorption spectra were recorded on a Perkin Elmer UV/Vis/NIR lambda 19 spectrometer. The measurements were done at thin films of the samples, prepared by rubbing them on a quartz surface.

Raman spectra were recorded on a FT-Raman spectrometer Bruker, RFS 100 equipped with the Nd-YAG laser 1064 nm NIR line. The power of the excitation radiation was 150mW

Theoretical calculations: The molecular geometry optimization and vibrational wavenumber calculations of the three compounds were performed by DFT method using the GAMESS package. The simulated spectrum is predicted by TD-DFT/B3LYP/SBK level of theory. GAMESS is a program for ab initio molecular quantum chemistry that can compute SCF wave functions ranging from RHF, ROHF, UHF, GVB and MCSCF [27], [28]. The Becke three-parameter hybrid exchange functional and the Lee–Yang–Parr correlation functional (B3LYP) were utilized in the

calculation. Calculations were carried out using the SBKJC basis with the SBKJC pseudopotential [29]. In order to take into account the effect of intermolecular interactions on geometrical parameters and vibrational spectroscopy, we have considered an appropriate cluster model built up from two $(\text{SbX}_5)_2^-$ ($X = \text{Cl}, \text{Br}, \text{I}$) anion and four $(\text{CH}_3\text{SC}(\text{NH}_2)_2)^+$ cations linked by N-H...X hydrogen bonds and Sb-X-Sb bonds (see Figure 1). All the parameters were allowed to relax and all the calculations converged to an optimized geometry which corresponds to an energy minimum as revealed by the lack of imaginary values in the calculated wavenumbers. The HOMO and LUMO molecular orbitals are analysed and drawn using CHEMISIAN program [30]. The vibrational modes were made by visual inspection of modes animated by using MOLDEN 3.8 program [31] and by comparison with the previous theoretical and experimental results reported in the literature for similar compounds.

Supporting Information (see footnote on the first page of this article): Crystal data, Tauc plots, IR and Raman spectra of all compounds.

Acknowledgements

This work is supported by The ENARET-MED-ENERG-11-132 project: "HYDROSOL". by the "Greek General Secretariat of Research and Technology" and by the Ministry of High Education of Tunisia.

Keywords: organic–inorganic hybrid composites · perovskite phases · crystal structure · theoretical calculations

- [1] C. R. Kagan, D. B. Mitzi, C. D. Dimitrakopoulos, *Science* **1999**, 286, 945-947.
- [2] W. Bi, N. Louvain, N. Mercier, J. Luc, I. Rau, F. Kajzar, B. Sahraoui, *Adv. Mater.* **2008**, 20, 1013-1017.
- [3] G. C. Papavassiliou, G. A. Mousdis, G. Pagona, N. Karousis, M.-S. Vidali, *J. Lum.* **2014**, 149, 287-291.
- [4] G. A. Mousdis, G. C. Papavassiliou, A. Terzis, C. P. Raptopoulou, *Z. Naturforsch.* **1998**, 53b, 927-931.
- [5] a) D. B. Mitzi, K. Chondroudis, C. R. Kagan, *Inorg. Chem.* **1999**, 38, 6246-6256; b) C. Hrzi, A. Samet, Y. Abid, S. Chaabouni, M. Fliyou, A. Koumina, *J. Mol. Struct.* **2011**, 992, 96-101; c) A. Samet, A. B. Ahmed, A. Mlayah, H. Boughzala, E. K. Hliil, Y. Abid, *J. Mol. Struct.* **2010**, 977, 72-77; d) Y.-J. Wang, L. Xu, *J. Mol. Struct.* **2008**, 875, 570-576; e) A. M. Goforth, M. D. Smith, L. Peterson Jr., H.-C. Zur Loye, *Inorg. Chem.* **2004**, 43, 7042-7049.
- [6] a) J. Burschka, N. Pellet, S. J. Moon, R. Humphry-Baker, P. Gao, M. K. Nazeeruddin, M. Gratzel, *Nature* **2013**, 499, 316-319; b) M. A. Green, A. Ho-Baillie, H. J. Snaith, *Nat. Photonics.* **2014**, 8, 506-514.
- [7] G. Xing, N. Mathews, S. Lim, N. Yantara, X. Liu, D. Sabba, M. Graetzel, S. Mhaisalkar, T. Sum, *Nat. Mater.* **2014**, 13, 476-480.
- [8] Z.-K. Tan, R. S. Moghaddam, M. L. Lai, P. Docampo, R. Higler, F. Deschler, M. Price, A. Sadhanala, L. M. Pazos, D. Credgington, F. Hanusch, T. Bein, H. J. Snaith, R. H. Friend, *Nat. Nanotechnol.* **2014**, 9, 687-692.
- [9] X. Y. Chin, D. Cortecchia, J. Yin, A. Bruno, C. Soci, *Nat. Commun.* **2015**, 6, 7383.
- [10] R. E. Brandt, V. Stevanovic, D. S. Ginley, T. Buonassisi, *MRS Commun.* **2015**, 5, 265-275.
- [11] B. Saparov, F. Hong, J.-P. Sun, H.-S. Duan, W. Meng, S. Cameron, I. G. Hill, Y. Yan, D. B. Mitzi, *Chem. Mater.* **2015**, 27, 5622-5632.
- [12] a) B.-W. Park, B. Philippe, X. Zhang, H. Rensmo, G. Boschloo, E. M. J. Johansson, *Adv. Mat.* **2015**, 27, 6806-6813; b) K. Eckhardt, V. Bon, J. Getzschmann, J. Grothe, F. M. Wieser, S. Kaskel, *Chem. Comm.* **2016**, 52, 3058-3060.
- [13] G. A. Fisher, N. C. Norman, *Adv. Inorg. Chem.* **1994**, 41, 233-271.
- [14] a) M. Gdaniec, Z. Kosturkiewicz, R. Jakubas, L. Sobczyk, *Ferroelectrics* **1988**, 77, 31-37; b) D. B. Mitzi, *Inorg. Chem.* **2000**, 39, 6107-6113.
- [15] G. A. Mousdis, V. Gionis, G. C. Papavassiliou, C. P. Raptopoulou, A. Terzis, *J. Mater. Chem.* **1998**, 8(10), 2259-2262.
- [16] a) M. A. Spackman, D. Jayatilaka, *Cryst Eng Comm* **2009**, 11, 19-32; (b) J. J. McKinnon, F. P. A. Fabbiani, M. A. Spackman, *Cryst. Growth Des.* **2007**, 7, 755-769; (c) J. J. McKinnon, M. A. Spackman, A. S. Mitchell, *Acta Crystallogr. B* **2004**, 60, 627-668; (d) K. Takahashi, N. Hoshino, T. Takeda, S. Noro, T. Nakamura, S. Takeda, T. Akutagawa, *Inorg. Chem.* **2015**, 54, 9423-9431; (e) M. A. Spackman, J. J. McKinnon, *Cryst. Eng. Comm.* **2002**, 4, 378-392.
- [17] a) A. Amat, E. Mosconi, E. Ronca, C. Quantì, P. Umari, Md. K. Nazeeruddin, M. Gratzel, F. De Angelis, *Nano Lett.* **2014**, 14, 3608-3616; b) J. H. Lee, J. H. Lee, E. H. Kong and H. M. Jang, *Sci. Rep.* , **2016**, 6, 21687..
- [18] a) J. Tarasiewicz, R. Jakubas, J. Zaleski, J. Baran, *J. Mol. Struct.* **2008** 876, 86-101; b) M. Bujak, *Polyhedron* **2015**, 85, 499-505..
- [19] J.E. Monat, J.H. Rodriguez, J.K. McCusker, *J. Phys. Chem. A* **2002**, 106, 7399-7406..
- [20] J. Tarasiewicz, R. Jakubas, J. Baran, A. Pietraszko, *J. Mol. Struct.* **2004**, 697, 161-171.
- [21] P. W. Jagodzinski, J. Laane, *J. Raman Spectr.* **1980**, 9, 22-27.
- [22] F. Cariati, A. Panzanelli, L. Antoilini, L. Menabue, G.C. Pellacani, G. Marcotrigiano, *J. Chem. Soc., Dalton Trans.* **1981**, 4, 909-913.
- [23] F. Cariati, G. Marcotrigiano, L. Menabue, F. Morazzoni, G.C. Pellacani, G. M. Zanderighi, *Spectrochim. Acta Part A* **1978**, 34, 801-805.
- [24] Rigaku/MS-Crystal Clear. Rigaku/MS-Crystal Clear, The Woodlands, Texas, USA. **2005**.
- [25] a) G. M. Sheldrick, *Acta Cryst.* **2008**, A64, 112-122. b) G. M. Sheldrick, *Acta Cryst.* **2015**, C71, 3-8. c) DIAMOND – *Crystal and Molecular Structure Visualization*, Ver. 3.1, Crystal Impact, Rathausgasse 30, 53111, Bonn, Germany.
- [26] S. K. Wolff, D. J. Grimwood, J. J. McKinnon, M. J. Turner, D. Jayatilaka, M. A. Spackman, *Crystal Explorer*, The University of Western Australia, Crawley, Australia, **2012**
- [27] " M. W. Schmidt, K. K. Baldrige, J. A. Boatz, S. T. Elbert, M. S. Gordon, J. H. Jensen, S. Koseki, N. Matsunaga, K. A. Nguyen, S. Su, T. L. Windus, M. Dupuis, J. A. Montgomery, *J. Comput. Chem.* **1993**, 14, 1347-1363.
- [28] M. S. Gordon, M. W. Schmidt pp. 1167-1189, in *Theory and Applications of Computational Chemistry: the first forty years* (Eds: C. E. Dykstra, G. Frenking, K. S. Kim, G. E. Scuseria), Elsevier, Amsterdam, **2005**.
- [29] N. P. Labello, A. M. Ferreira, H. A. Kurtz, *J. Comput. Chem.* **2005**, 26, 1464-1471.
- [30] <http://www.chemissian.com/>
- [31] J. H. Noordik, G. J. Schaftenaar, *Comput. Aided Mol. Des.* **2000**, 14, 123-134.

Entry for the Table of Contents (Please choose one layout)

FULL PAPER



The novel organic–inorganic hybrid compounds of the general formula $[\text{CH}_3\text{SC}(\text{NH}_2)_2]_2\text{SbA}_5$, were successfully synthesized. Their structure consists of corner sharing SbA_6 octahedra forming zigzag chains with the amine located in the free cavities between chains. Their structure, optical and vibronic properties were studied. DFT calculations were made in order to compare the results with the experimental findings and gain an insight of the properties of these new compounds.

Key Topic: organic–inorganic hybrid composites based on Sb

G. A. Mousdis N. – M. Ganotopoulos, H. Barkaoui, Y. Abid, V. Psycharis, A. Savvidou and C.e P. Raptopoulou*

Page No. – Page No.

Title: Preparation and Characterization of some new one-dimensional organic-inorganic hybrid materials based on Sb